Mem. S.A.It. Vol. 93, 236

Memorie della

Next Generation X-ray Imaging Surveys

R. Gilli[1], M. Ghigo[2], S. Marchesi[1], G. Lanzuisi[1], S. Ettori[1], A. Comastri[1], F. Vito[3,1], G. Pareschi[2], M. Civitani[2], S. Basso[2], B. Salmaso[2], G. Vecchi[2], C. Vignali[4,1], M. Brusa[4,1], P. Rosati[5,1], P. Tozzi[6], S. Borgani[7,8,9,10], M. Paolillo[11,12,13]

[1] INAF – Osservatorio di Astrofisica e Scienza dello Spazio di Bologna, Via P. Gobetti 93/3, 40129 Bologna, Italy, e-mail: roberto.gilli@inaf.it
[2] INAF – Osservatorio Astronomico di Brera, Via Bianchi 46, 23807 Merate, Italy
[3] Scuola Normale Superiore, Piazza dei Cavalieri 7, 56126 Pisa, Italy
[4] Dipartimento di Fisica e Astronomia, Università degli Studi di Bologna, Via P. Gobetti 93/2, 40129 Bologna, Italy
[5] Dipartimento di Fisica e Scienze della Terra, Università degli Studi di Ferrara, Via G. Saragat 1, 44122 Ferrara, Italy
[6] INAF – Osservatorio Astrofisico di Arcetri, Largo E. Fermi 5, 50125 Firenze, Italy
[7] Dipartimento di Fisica, Univ. Università degli Studi di Trieste, Via G.B. Tiepolo 11, 34143 Trieste, Italy
[8] INAF – Osservatorio Astronomico di Trieste,Via G. B. Tiepolo 11, 34143 Trieste, Italy
[9] IFPU - Institute for Fundamental Physics of the Universe, via Beirut 2, I-34014, Trieste, Italy
[10] INFN – Sezione di Trieste, Trieste, Italy
[11] Dipartimento di Fisica “Ettore Pancini”, Università Federico II, Via Cinthia, 80126 Napoli, Italy
[12] INAF – Osservatorio Astronomico di Capodimonte, Via Moiariello 16, 80131 Napoli, Italy
[13] INFN – Sezione di Napoli, Napoli, Italy

Received: 31 December 2021; Accepted: 29 May 2022

Abstract. The launch of Chandra more than twenty years ago marked a turning point in our understanding of the deep X-ray Universe. The 0.1 deg^2 Chandra Deep Field South (CDFS), the 2 deg^2 Chandra-COSMOS Legacy, and the other Chandra deep fields have probed the physics and evolution of distant supermassive black holes to a level that is as yet unsurpassed. Chandra's sub-arcsec angular resolution is at the basis of its exquisite sensitivity. Yet, its low collecting area and limited field of view allowed deep X-ray exploration of small sky areas only. Substantial advances in the development of lightweight X-ray optics with large photon-collecting area, large field of view, and sharp angular resolution are required to overcome Chandra's limits and bring the discovery space of deep X-ray surveys to the equivalent of hundreds-to-thousands of Chandra deep fields.
We here describe our contribution to the development of the leading technology for building lightweight optics with sharp angular resolution and to the definition of the survey science for the next-generation X-ray imaging facilities STAR-X and AXIS.

Key words. X-rays: general – galaxies – surveys – telescopes – galaxies: active

1. The STAR-X and AXIS concepts

This project was primarily aimed to support the development of the Survey and Time-domain Astrophysical Research eXplorer (STAR-X; Zhang et al. 2017) mission concept that we joined in 2015 and was submitted to NASA in 2016 in response to a call for medium explorer (MIDEX) missions[1]. STAR-X was largely based on the Wide Field X-ray Telescope concept (WFXT[2]; Rosati et al. 2011) that was submitted to the US Astro2010 Decadal Survey[3] (Giacconi et al. 2009; Murray et al. 2009; Vikhlinin et al. 2009; Ptak et al. 2009), and to which our team contributed extensively. Similarly to WFXT, the STAR-X concept was featuring a unique combination of: i) wide field of view (1 deg^2); ii) large effective area (>1800 cm^2 at 1 keV); iii) excellent and uniform point spread function over the entire field of view (~5 arcsec Half Power Diameter, HPD[4]); iv) low detector background. In addition, it featured a fast-slewing spacecraft bus. STAR-X was expected to conduct wide-area (thousands of deg^2) surveys of legacy fields with extensive multi-wavelength coverage. Unlike previous X-ray surveys, STAR-X's observations were meant to be conducted with a cadence designed to discover faint transient sources (tidal disruption flares, supernova shock breakouts, outbursting black holes) at a 10-100× higher rate than that of all current X-ray missions. STAR-X was then expected to fill a critical wavelength and scientific gap between current X-ray observatories, such as Chandra, XMM and eROSITA[5], and the launch of Athena[6] in the ~2030. It aimed to provide well-matched – in terms of both sensitivity and surveyed area - X-ray coverage when the astronomical landscape will be dominated by wide-area multi-wavelength imaging surveys. The mission's single instrument, the X-ray Telescope Assembly, consists of a mirror assembly and CCD detectors. The baseline enabling technology, primarily developed by NASA/GSFC, is lightweight single-crystal silicon directly-polished optics to be assembled into meta-shells (see Fig. 1 *left*; Zhang et al. 2017; McClelland 2017). This approach is extremely promising: angular resolutions of <4 arcsec HPD on a 2-reflection mirror have been already measured in X-rays, and the possibility to improve the profile via ion-figuring correction at resolution < 1 arcsec has been shown with metrological data (Riveros et al. 2017).

On September 2017 the results of the 2016 NASA MIDEX call were issued: three mission concepts were selected for a Phase A study. STAR-X ranked 4th and was therefore not selected. The mirror technology at the basis of the STAR-X concept, as well as a large part of the science team, migrated into a new mission concept called the Advanced X-ray Imaging Satellite (AXIS[7]; Mushotzky 2018; Mushotzky et al. 2019), a study for a larger, probe-class mission with high-resolution optics and flat, sub-arcsec PSF over FoV commissioned by NASA for the US Astro2020 Decadal Survey[8].

AXIS is designed to have a stable, sub-arcsec resolution over a 24′×24′ field of view: this would be an improvement by a factor of ~50 in solid angle with respect to Chandra, which only has sub-arcsec resolution at off-axis angles <2′. The observing bandpass is 0.3-10 keV and the total effective area is about 7000 cm^2 at 1 keV (Fig. 1 *right*). AXIS is planned to have a remarkably low detector background, thus increasing sensitivity to extended sources, and high observing efficiency.

On November 2021 the Astro2020 Decadal Survey report was released and listed among its priorities *'a targeted X-ray probe that complements ESA's Athena mission'* for a possible launch in ~2030. AXIS perfectly matches this requirement, but key technology steps are needed to bring the resolution of a single mirror segment significantly below 0.5" HPD and

[1] https://explorers.larc.nasa.gov/APMIDEX2016/
[2] http://sait.oat.ts.astro.it/MSAIS/17/index.html
[3] https://science.nasa.gov/astrophysics/special-events/astro2010-astronomy-and-astrophysics-decadal-survey
[4] Also known as Half Energy Width, HEW.
[5] https://www.mpe.mpg.de/eROSITA
[6] https://www.the-athena-x-ray-observatory.eu/
[7] https://axis.astro.umd.edu/
[8] https://www.nationalacademies.org/our-work/decadal-survey-on-astronomy-and-astrophysics-2020-astro2020

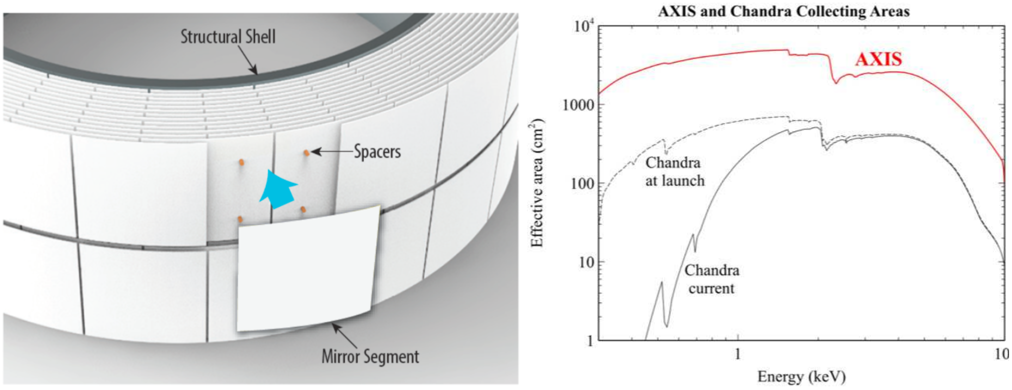

Fig. 1. *Left:* Mirror concept at the basis of proposed next-generation X-ray imaging missions like STAR-X and AXIS. Individual mirror segments are integrated into meta-shells to provide lightweight X-ray optics with large-collecting area. From McClelland (2017). *Right:* Expected AXIS collecting area including detector efficiency and filters compared to that of Chandra at launch and as of 2018. From Mushotzky (2018).

to produce the breadboards of the mirror assembly.

In parallel, the mirror development targeted the new, 2021 NASA call for a MIDEX mission to be launched in ~2026. The STAR-X 2016 team rearranged and a new, revisited STAR-X concept was just submitted (Dec 9th, 2021) to the 2021 MIDEX call. Its technical requirements were similar, but not identical, to those of the 2016 concept. Also, the science goals were revisited, and a new, primary science case added, that is, the understanding of how large scale structures form and evolve at early epochs, e.g. $z > 2$, through the direct detection of the hot ICM in distant protoclusters, and of the accreting SMBHs populating those structures and their feedback effects. The main technical goal of the STAR-X 2021 mission is to achieve a stable PSF of 2.5-3 arcsec HPD within 0.2 deg^2, and < 6" averaged over the entire 1 deg^2 FoV. This will represent a revolution for X-ray surveys, as originally envisaged with the WFXT concept. For comparison, Chandra has 3" HPD average over 0.08 deg^2, XMM and eROSITA 30" HPD over 0.2 deg^2 and 1 deg^2, respectively. This meta-shell technology has the potential to become the benchmark for X-ray lightweight optics fabrication in the next decades and is, in fact, the current baseline mirror technology even for the US strategic mission concept *Lynx*[9] (The Lynx Team 2018).

2. Simulations and definition of the science case

Some of the science definition activities that our group originally planned for STAR-X were re-focused on AXIS. In particular, we contributed to the definition of the following scientific cases: 1) the search for accreting super-massive black holes at redshifts 6 and above in a multi-tiered survey, and 2) the physics of galaxy clusters. These contributions were partly included in the AXIS white paper submitted to the NASA Astro2020 Decadal Survey (Mushotzky et al. 2019). The AGN survey science was then extensively discussed in Marchesi et al. (2020). In that paper, we presented a series of mock catalogs of X-ray selected active galactic nuclei (AGNs), non-active galaxies, and galaxy clusters that were based on up-to-date observational results on the demographic of extragalactic X-ray sources and their extrapolations. The mocks reach fluxes below 10^{-20} erg cm^{-2} s^{-1} in the 0.5-2 keV band, that is, more than an order of magnitude below the anticipated limit of even the deepest future fields (e.g. with *Lynx*). They

9 https://www.lynxobservatory.com/

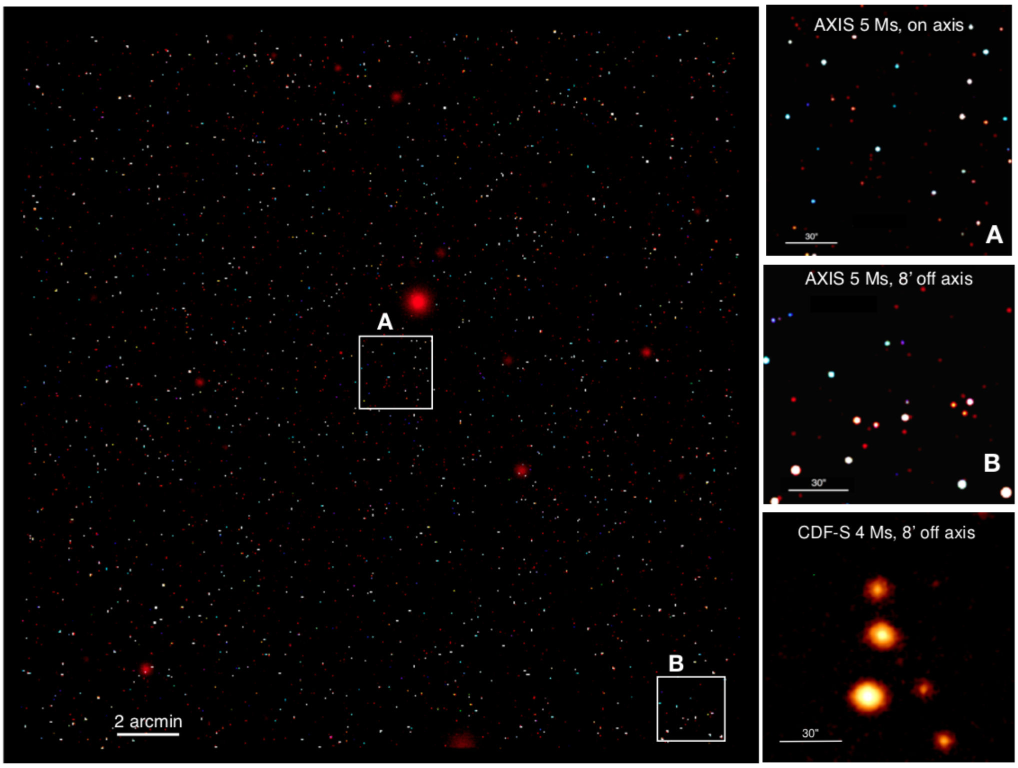

Fig. 2. *Left*; Smoothed three-color image (red: 0.5-2 keV; green: 2-4.5 keV blue: 7 keV) of a simulated 5-Ms deep field (24′x24′) with AXIS. The extended red structures are galaxy clusters. The white boxes highlight two regions, one on-axis and the one at the boundary of the field of view: we show a zoom-in of these regions in the top- and central-right panels. The AXIS PSF is expected to have remarkably small degradation as a function of the off-axis angle. In the bottom right panel, we show as a reference a ∼2′x2′, 8′ off-axis 0.5–7 keV image of the 4 Ms CDF-S. From Marchesi et al. (2020).

represent an important tool for simulating extragalactic X-ray surveys with a large suite of current and future telescopes and have been made publicly available[10].

We used our mocks to perform a set of end-to-end simulations of X-ray surveys with AXIS, finding that they may transform our knowledge of the deep X-ray Universe. As an example, in a total observing time of 15 Ms, AXIS would be able to detect ∼225,000 AGNs and ∼50,000 non-active galaxies, reaching a flux limit of $\sim 5 \times 10^{-19}$ erg cm^{-2} s^{-1} in the 0.5-2 keV band, with an improvement of over an order of magnitude with respect to surveys with current X-ray facilities. Consequently, 90% of these sources would be detected for the first time in the X-rays.

[10] See: http://cxb.oas.inaf.it/mock.html

The strawman survey plan for AXIS is made by three layers: i) a deep, pencil-beam survey made by a single pointing (∼0.16 deg^2); ii) a 2.5 deg^2 moderate–depth survey with 300 ks uniform exposure; iii) a 50 deg^2 shallower survey with 15ks uniform exposure. Each layer will then be observed for 5Ms. Based on this reference plan, we used the mock catalogs mentioned above and the Monte Carlo code Simulation of X-ray Telescopes (SIXTE; Dauser et al. 2019) to generate simulated AXIS surveys. We fed SIXTE with the AXIS configuration files (i.e., telescope setup, response matrices, vignetting, point spread function, detec-

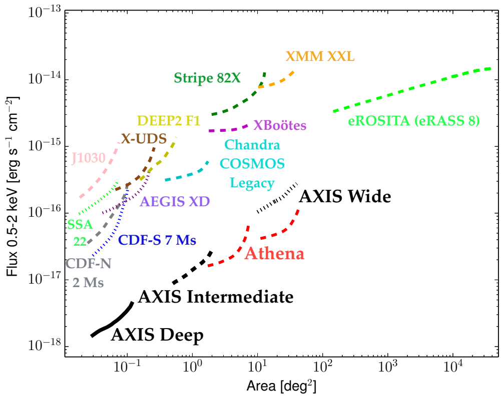

Fig. 3. 0.5–2 keV area-flux curves for the three AXIS surveys (black curves) compared with those of the major existing X-ray surveys. The predictions for the *Athena* surveys (with 5” HPD, red curves), and those for the four years of eROSITA observations (i.e., eRASS:8; Merloni et al. 2012; Comparat et al. 2019, dashed light green line) are also shown. The plotted curves have been derived from the 0.5-2 keV survey sensitivity curves in an area range that starts at 20% and stops at 80% of the area covered by the survey. From Marchesi et al. (2020).

tor background) and produced a set of AXIS images of the sky using different exposure times. The simulated deep layer of the survey (i.e. a single 5Ms AXIS tile) is shown in Fig. 2.

We then run the wavdetect detection algorithm on all simulated images and compared the ratio between the number of input vs the output sources as a function of their flux to estimate the completeness and reliability of the detections, and, ultimately, the survey sky-coverage. The sky-coverage of the three AXIS surveys is shown in Fig. 3 together with that of the main existing X-ray surveys. The expected sky coverage of the final eROSITA surveys (Merloni et al. 2012; Comparat et al. 2019), and of the Athena surveys are also shown. To allow a proper comparison with Athena, we produced simulated Athena surveys using the current requirement on angular resolution (5” HPD on-axis) and mission observing plan (as of Nov 2021, see Marchesi et al. 2020 for details) and following the same end-to-end approach used to generate the simulated AXIS surveys. Overall, AXIS is expected to return fewer but fainter X-ray sources than Athena. As shown in the next Section, AXIS is expected to open a new discovery space on early SMBHs and put strong constraints to their formation and growth mechanisms.

2.1. High-redshift AGN

The predictions on the number of high-z sources to be discovered by AXIS are based on mock catalogs generated using the XLFs of AGN at z=3-5 in Vito et al. (2014). These XLFs provide the best representation to date of the faintest X-ray AGN populations probed by the 7Ms CDFS observation (Vito et al. 2018).

At $z > 3$, AXIS is expected to detect ~350, ~2000, and ~6700 AGNs in the deep, medium and wide area survey, respectively. This would be a major leap forward with respect to currently available X-ray datasets. For example, the 7Ms CDFS, contains ~70 $z > 3$ AGNs (Vito et al. 2018) over an area of ~330 arcmin^2; the 2.2 deg^2 Chandra COSMOS Legacy survey, which required an overall 4.6 Ms Chandra exposure, contains 174 $z > 3$ AGNs (Marchesi et al. 2016); and the 31 deg^2 Stripe 82X survey, which combined ~500 ks of Chandra time and ~1 Ms of XMM time for an overall 1.5 Ms X-ray exposure, contains 45 $z > 3$ (Ananna et al. 2017). Even more importantly, the AXIS surveys would allow us to detect for the first time a population of *X-ray-selected* $z > 6$ *AGN*: we expect to detect a total of ~100 of these primordial accreting supermassive black holes from the three surveys. If the predictions of the Vito et al. (2014) XLF are confirmed, we also expect to detect sources up to z ~8, possibly enabling the direct detection of late-stage accreting SMBHs seeds. We recall that none of the AGN at $z > 6$ known to date have been discovered through X-ray selection.

In Fig. 4 (*left*), we plot the AGN 0.5–2 keV luminosity as a function of redshift for the AXIS and Athena z >3 samples. While Athena will collect more sources, AXIS is expected to sample luminosities ~1 dex fainter up to redshift ~8, highlighting the complementarity between the two instruments. In the same figure we also report the evolution with redshift of the X-ray luminosity of two idealized BHs

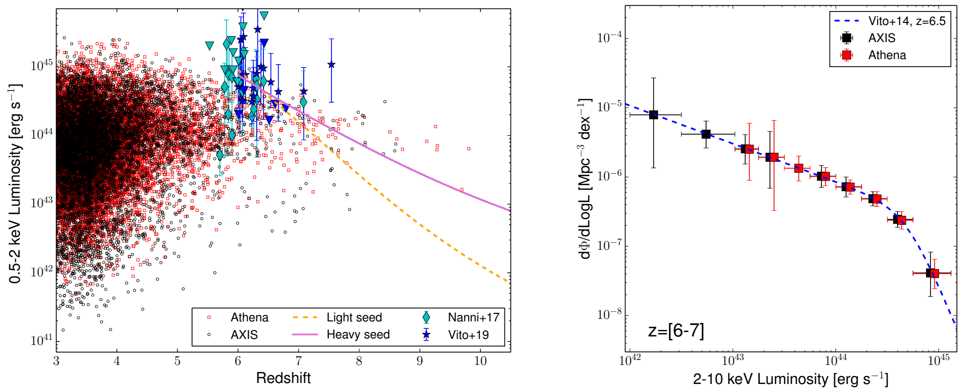

Fig. 4. *Left:* X-ray luminosity vs redshift distribution of $z > 3$ AGN detected in the simulated AXIS (black circles) and Athena (red squares) surveys. The on-axis HPD assumed for the AXIS and Athena pointings is 0.5" and 5", respectively. The $z > 5.5$ QSOs detected in the X-rays by currently available facilities are also plot for comparison (Vito et al. 2019, blue stars; Nanni et al. 2017, cyan diamonds). Two possible tracks for the progenitors of known, luminous $z \sim 6$ QSOs are also shown. These are based on two different BH seed models (light SMBH seed: dashed yellow line; heavy SMBH seed: solid magenta line; see the text for details). *Right:* AGN X-ray luminosity function at $z = [6-7]$ as expected to be measured by AXIS (black points) and Athena (red points). The model $z = 6.5$ XLF from Vito et al. (2014) is plotted as a blue dashed line. From Marchesi et al. (2020).

growing to Log($M_{BH}/M_{\odot}$)=9.1 at z=6 through continuous accretion. Such large SMBHs are commonly found to power luminous ($L_X \sim 10^{45}$ erg s^{-1}) quasars at z=6 in current wide-area optical surveys, such as the SDSS (Fan 2006) and PanSTARRS (Bañados et al. 2016). The two curves refer to two models of BH accretion at a fixed Eddington ratio, starting from either a $10^2\ M_{\odot}$ or $10^5\ M_{\odot}$ seed (see Marchesi et al. 2020 for details). These growth models are oversimplified, but in principle next generation X-ray surveys would have the sensitivity to detect the progenitors of SDSS QSOs. Remarkably, owing to the significant obscuration that may affect BH accretion in its earliest phases (Ni et al. 2020; Lupi et al. 2021), X-ray surveys are expected to be the best way to discover the progenitors of $z \sim 6$ QSOs.

In Fig. 4 (*right*), we show the XLF of AGN at z=[6-7] as it will be measured by AXIS and Athena. AXIS is expected to probe X-ray luminosities down to 10^{42} erg s^{-1} at $z \gtrsim 6$, that is ~1 dex lower than Athena. At those redshifts, the expectations of theory are uncertain by 2 dex or more, and AXIS measurements will provide unique observational constraints to the models of formation and growth of early SMBHs.

3. Mirror development

Besides the definition of the survey science of next-generation X-ray imaging missions, our group contributed significantly to improve the readiness of the mirror technology through the ion-beam figuring (IBF) correction (Pareschi et al. 2016; Civitani et al. 2017) of single mirror segments provided by GSFC. A series of tests on the shape correction of silicon X-ray mirrors have been performed using the IBF facilities available at INAF-Brera. A representative result obtained on a mono-crystalline silicon mirror previously figured provided by NASA/GSFC is shown in Fig. 5. The sample size was 80 mm × 100 mm and 0.76mm thick, with a sagittal radius of 150 mm. For the performed tests, the ion-figuring removal rate obtained on the Silicon was of 4.5 nm/sec and the overall size of the Removal Function was 28mm with a FWHM of 9mm. The shell

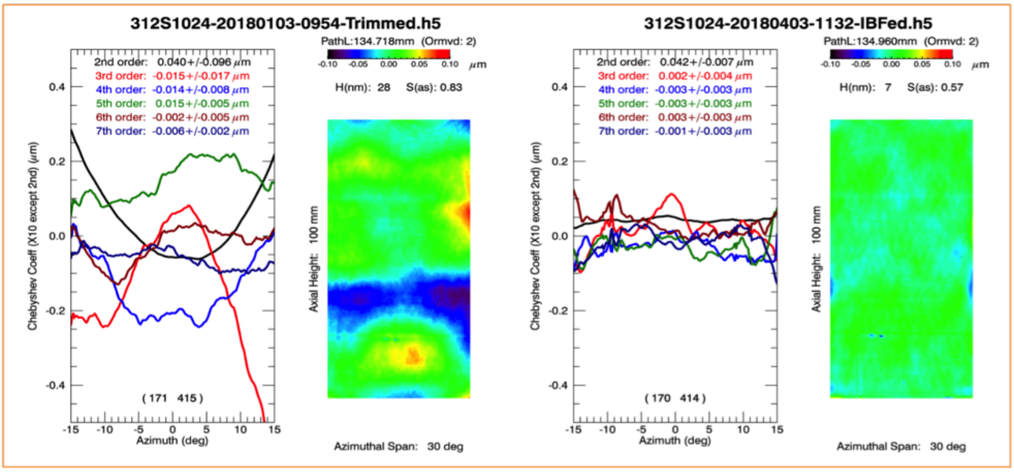

Fig. 5. Mirror sample before (left) and after (right) ion-beam figuring at INAF-Brera. From Ghigo et al. (2018).

was mounted on a curved support made of aluminum fixed on the holder that keeps the samples in vertical position during the ion-figuring process. A good thermal contact between shell and aluminum was obtained using a temperature resistant vacuum grease produced by the Apiezon company. This was necessary to dissipate the heat during the figuring. Three small holding fingers made in graphite were used in order to safely fix the shell. During the figuring run, that lasted 1.6 hours, the temperature of the aluminum block reached a peak of 35 ^{o}C, a sufficiently low temperature to guarantee a small thermal impact on the substrates and, consequently, a low stress level.

The initial map of the shell containing the errors to be corrected was provided by NASA/GSFC and is shown in Fig. 5 (*left*). After the ion-figuring, the shell was sent back to GSFC for measuring the result of the correction test. A good improvement of the overall figure was obtained (Fig. 5 *right*): the shape error was reduced by a factor of 4, i.e. from 28 nm to 7 nm. An improvement of the low-spatial-frequency errors at length scale $>$ 10 mm was also observed (Fig. 6 *left*). As expected, the mid-to-high-frequency errors did not show any change, as the FWHM size of 9 mm of the Removal Function is unable to correct them. Also the micro-roughness of the surface did not increase after the ion-figuring process (Fig. 6 *right*).

This shell will be a single element of a pair of mirrors (parabola-hyperbole) placed in series. Also the other complementary shell segment was then figured. The simulation result for the two Silicon mirrors, corrected and properly aligned, gave the estimation that the pair can produce images with an HPD of about 1.5" at 1 keV. The Sagittal depth of the two mirrors (accounting for null lens calibration) are:

- Expected: 98 nm.
- Sample 312P1052: (95 +/- 14) nm.
- Sample 312S1024: (84 +/- 14) nm.
- Combined sag error: 17 nm (0.27" HPD).

These results, published in Ghigo et al. (2018), demonstrate that Ion Beam figuring can improve substantially the figure of the X-ray optics without worsening their micro-roughness.

4. Conclusions

A new set of deep-and-wide X-ray imaging surveys with the discovery potential of hundreds-to-thousands of Chandra deep fields is key to produce major advances in our under-

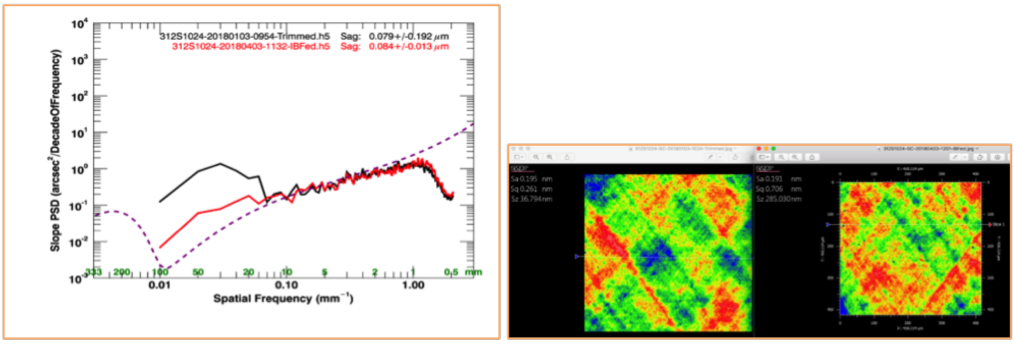

Fig. 6. *Left:* PSD before (black) and after (red) ion-beam figuring. From Ghigo et al. (2018). *Right:* Micro-roughness of the mirror surface before (left) and after (right) the figuring.

standing of how SMBHs and large-scale structures form and evolve in the early Universe, and to match the survey capabilities of optical, IR and radio facilities operating in the 2030-2040s. To perform such next-generation X-ray surveys, next-generation X-ray mirrors are required, but building them is challenging. They in fact need to have large photon-collecting area, large field of view, sharp angular resolution, and be at the same time lightweight. The project funded by the ASI-INAF agreement allowed us to i): develop sophisticated and realistic end-to-end simulations to define the survey science of STAR-X and AXIS, a new medium- and probe-class X-ray imaging mission concept, respectively; ii): contribute to the development of the meta-shell technology, i.e. the leading technology for building lightweight optics with sharp angular resolution at the bases of next-generation X-ray imaging missions; iii) ultimately maintain INAF involvement in the above mentioned projects under evaluation at NASA.

Acknowledgements. All the activities presented in this contribution have been funded in the framework of the ASI/INAF agreement n. 2017-14-H.O *"Attività di Studio per la comunità di astrofisica delle alte energie e fisica astro-particellare. Bando: Nuove missioni scientifiche"*, through the project *"STAR-X: the next generation of X-ray imaging surveys"*.

References

Ananna, T. T., Salvato, M., LaMassa, S., et al. 2017, ApJ, 850, 66
Bañados, E., Venemans, B. P., Decarli, R., et al. 2016, ApJS, 227, 11
Civitani, M. M., Hołyszko, J., Vecchi, G., et al. 2017, in Society of Photo-Optical Instrumentation Engineers (SPIE) Conference Series, Vol. 10399, Society of Photo-Optical Instrumentation Engineers (SPIE) Conference Series, 103990W
Comparat, J., Merloni, A., Salvato, M., et al. 2019, MNRAS, 487, 2005
Dauser, T., Falkner, S., Lorenz, M., et al. 2019, A&A, 630, A66
Fan, X. 2006, New Astronomy Review, 50, 665
Ghigo, M., Basso, S., Civitani, M., et al. 2018, in Society of Photo-Optical Instrumentation Engineers (SPIE) Conference Series, Vol. 10706, Advances in Optical and Mechanical Technologies for Telescopes and Instrumentation III, ed. R. Navarro & R. Geyl, 107063I
Giacconi, R., Borgani, S., Rosati, P., et al. 2009, in astro2010: The Astronomy and Astrophysics Decadal Survey, Vol. 2010, 90
Lupi, A., Haiman, Z., & Volonteri, M. 2021, arXiv e-prints, arXiv:2102.05051
Marchesi, S., Civano, F., Salvato, M., et al. 2016, ApJ, 827, 150
Marchesi, S., Gilli, R., Lanzuisi, G., et al. 2020, A&A, 642, A184
McClelland, R. S. 2017, in Society of Photo-Optical Instrumentation Engineers (SPIE) Conference Series, Vol. 10399, Society of Photo-Optical Instrumentation Engineers

(SPIE) Conference Series, 1039908
Merloni, A., Predehl, P., Becker, W., et al. 2012, arXiv e-prints, arXiv:1209.3114
Murray, S., Gilli, R., Tozzi, P., et al. 2009, in astro2010: The Astronomy and Astrophysics Decadal Survey, Vol. 2010, 217
Mushotzky, R. 2018, in Society of Photo-Optical Instrumentation Engineers (SPIE) Conference Series, Vol. 10699, Space Telescopes and Instrumentation 2018: Ultraviolet to Gamma Ray, ed. J.-W. A. den Herder, S. Nikzad, & K. Nakazawa, 1069929
Mushotzky, R., Aird, J., Barger, A. J., et al. 2019, in Bulletin of the American Astronomical Society, Vol. 51, 107
Nanni, R., Vignali, C., Gilli, R., Moretti, A., & Brandt, W. N. 2017, A&A, 603, A128
Ni, Y., Di Matteo, T., Gilli, R., et al. 2020, MNRAS, 495, 2135
Pareschi, G., Basso, S., Civitani, M. M., et al. 2016, in Society of Photo-Optical Instrumentation Engineers (SPIE) Conference Series, Vol. 9905, Space Telescopes and Instrumentation 2016: Ultraviolet to Gamma Ray, ed. J.-W. A. den Herder, T. Takahashi, & M. Bautz, 99051T
Ptak, A., Feigelson, E., Chu, Y. H., et al. 2009, in astro2010: The Astronomy and Astrophysics Decadal Survey, Vol. 2010, 240
Riveros, R. E., Biskach, M. P., Allgood, K. D., et al. 2017, in Society of Photo-Optical Instrumentation Engineers (SPIE) Conference Series, Vol. 10399, Society of Photo-Optical Instrumentation Engineers (SPIE) Conference Series, 103990T
Rosati, P., Borgani, S., Gilli, R., et al. 2011, Memorie della Societa Astronomica Italiana Supplementi, 17, 8
The Lynx Team. 2018, arXiv e-prints, arXiv:1809.09642
Vikhlinin, A., Murray, S., Gilli, R., et al. 2009, in astro2010: The Astronomy and Astrophysics Decadal Survey, Vol. 2010, 305
Vito, F., Brandt, W. N., Bauer, F. E., et al. 2019, A&A, 628, L6
Vito, F., Brandt, W. N., Yang, G., et al. 2018, MNRAS, 473, 2378
Vito, F., Gilli, R., Vignali, C., et al. 2014, MNRAS, 445, 3557
Zhang, W. W., Allgood, K. D., Biskach, M. P., et al. 2017, in Society of Photo-Optical Instrumentation Engineers (SPIE) Conference Series, Vol. 10399, Society of Photo-Optical Instrumentation Engineers (SPIE) Conference Series, 103990S